

# Controlling Non-Synchronous Microgrids for Load Balancing of Radial Distribution Systems

Tianqi Hong, *Student Member, IEEE*, and Francisco de León, *Fellow, IEEE*

**Abstract**—This paper proposes a novel control strategy such that downstream non-synchronous microgrids can perform load balancing functions. The proposed method can eliminate (or reduce) the unbalance of currents at the substation transformer of radial distribution systems. The load balancing ability of microgrids has been studied for two different scenarios: 1) using communications between the microgrid and the substation; and 2) using only local measurements at the microgrid. The limitations posed by the availability of measurements and system topology requirements for the success of the process are discussed. Two numerical examples are provided to validate the proposed control scheme using time domain and time-sequence power-flow simulations.

**Index Terms**—Distribution systems, load balancing, microgrid, smart grid.

## I. INTRODUCTION

**E**VEN THOUGH utilities intend to supply balanced voltage to their customers, voltage unbalance is a very common phenomenon in large distribution systems. Due to the unbalanced nature of power demands, the three-phase currents of downstream lines are unbalanced and therefore the voltages at the buses are also unbalanced. Unbalanced currents reduce the efficiency of the system and accelerate the aging process of transformers [1], [2].

In the past decades, numerous methods have been proposed to ease the current unbalance in distribution systems [1]–[8]. They all use system reconfiguration to balance the load. Typically, they are implemented using two approaches: load reduction and system structure reconfiguration.

Load reduction is a straightforward idea. To balance the demand, the unbalanced parts of the loads are supplied from different sources or Distributed Generation (DG) [3], [4], for example doubly fed induction generators [5], [6]. With DG the unbalanced loads seem to “disappear” from the grid.

System structure reconfiguration can be applied in two ways: static reconfiguration and dynamic reconfiguration. Static reconfiguration is a method based on static programming. Utilities are able to rearrange the distribution system to

balance the load according to a system static model (i.e., power flow). One way to implement static reconfiguration is phase swapping; see [1], [7]. A distribution system can be roughly balanced by migrating loads from a heavy loaded phase to a light loaded phase. The other approach is to reconfigure the system interconnecting difference phases through passive impedances [8]. The upstream system can be balanced by designing passive interconnections between different phases. However, the static reconfiguration method needs an accurate model of the target system. Once the system is modified, say the load changes, utilities need to re-analyze the modified system and implement the reconfiguration again.

The method of [8] can also be implemented as a dynamic reconfiguration approach by substituting the passive interconnection with power electronics devices. Hence, with dynamic reconfiguration the system can be balanced according to instantaneous measurements of the distribution system [9].

All the methods mentioned above need large investments. At the mega-Watt level DG and power electronics devices for dynamic reconfiguration are quite expensive. System level static reconfiguration is a big construction project and lacks of accuracy.

This paper puts forward the idea that to solve the unbalance problem, existing non-synchronous microgrids (NSMGs) offer a promising solution when adequately controlled. Due to the flexibility of NSMGs, there is a tendency to install NSMGs into distribution systems to improve power quality, system reliability, and resiliency [10]–[13]. In the literature, NSMGs are known for their ability to regulate their currents to three-phase balanced sinusoidal waves even when working under severe conditions, such as unbalanced loads or unbalanced and distorted voltages [14], [15].

In this paper, a novel control strategy is proposed for NSMGs to provide load balancing functions. Instead of balancing the microgrid currents, the NSMG is operated in a way to demand unbalanced currents aimed to negate the unbalance conditions of the system. In other words, the NSMG are operated unbalanced to balance the currents at the substation transformer. By applying the proposed control strategy to an existing NSMGs installed downstream in a distribution system, the expenses of implement load balancing functions is minimal.

Steady-state time-sequence power-flow simulations and transient analyses are used to validate the innovative control strategy for NSMGs. Simulations are performed using OpenDSS [16] for steady-state studies and Matlab Simulink for time-domain studies.

Manuscript received July 10, 2015; revised September 13, 2015 and December 13, 2015; accepted February 16, 2016. Paper no. TSG-00761-2015.

The authors are with the Department of Electrical and Computer Engineering, New York University, Brooklyn, NY 11201 USA (e-mail: th1275@nyu.edu; fdeleon@nyu.edu).

Color versions of one or more of the figures in this paper are available online at <http://ieeexplore.ieee.org>.

Digital Object Identifier 10.1109/TSG.2016.2531983

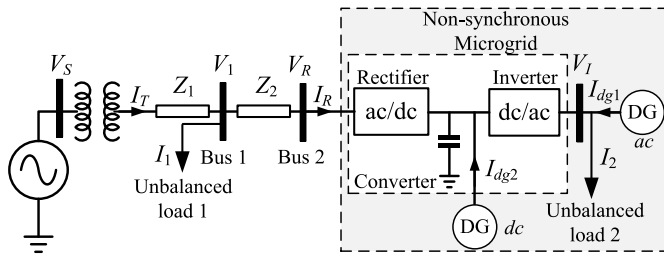


Fig. 1. Simplified structure of a radial distribution system with a non-synchronous microgrid and including DG.

## II. SYSTEM STRUCTURE

A simplified radial distribution network with a non-synchronous microgrid is shown in Fig. 1. The substation (high) voltage  $V_S$  in Fig. 1 is considered balanced. The unbalanced load 1 is an equivalent load for all loads other than unbalanced load 2 supplied from the microgrid. The substation supplies unbalanced load 1 through line impedance  $Z_1$  (which includes the transformer impedance) and load 2 is supplied by the substation and distributed generation (DG). When the capacity of DG is smaller than the total demand of load 2, load 2 and DG can be merged as an equivalent load. If the capacity of DG is larger than the load 2, the NSMG can be seen as a programmable load with negative resistance. In the following discussion, all DG inside the microgrid are merged with the microgrid load. In normal operation, the rectifier is controlled to absorb balanced current  $I_R$  and the inverter behaves as an ideal voltage source with balanced three-phase voltage output  $V_I$  to supply unbalanced load 2. Because of the unbalanced current  $I_1$  and line impedance  $Z_1$ ,  $V_1$  becomes unbalanced. Similarly, the input voltage to the rectifier  $V_R$  is unbalanced.

The three-phase currents of the rectifier  $I_R$  only have positive sequence component which is not helpful for reducing the current unbalance at the substation transformer. However, a proper control can be applied to the non-synchronous microgrid to eliminate (or reduce) the current unbalance problem.

## III. CONTROL OF NON-SYNCHRONOUS MICROGRID

The control policies of converter (dc-link) in the NSMG have been studied exhaustively [14]–[16]. A typical primary control strategy [16] existing in the literature is the two-loop feedback control, current and voltage loops, which has been applied to both rectifier and inverter of the NSMG. A brief description of the current control loop for unbalanced operation is presented next. Islanded operation is not considered in this paper. With a single current feedback loop control, the currents of the rectifier and currents of the inverter can be adjusted by tuning their references. The current references selection policies are provided in Section IV.

The common control block diagram is shown in Fig. 2.  $v_a, v_b$  and  $v_c$  are the three-phase instantaneous input voltage measurements of the converter. They are unbalanced and can be decomposed into three (balanced) sequence components using the conventional symmetrical components transformation.  $v_{abc}^+, v_{abc}^-$ , and  $v_{abc}^0$  are denoted as three-phase positive

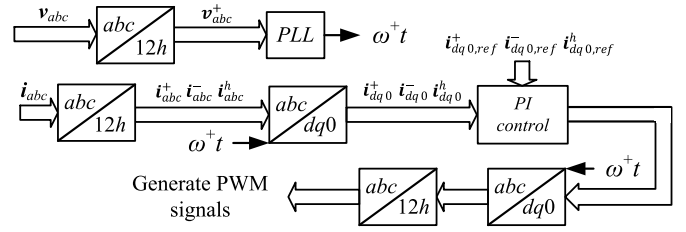


Fig. 2. Common control block diagram of a rectifier or inverter.

sequence, negative sequence, and zero sequence voltages. The positive sequence voltages are selected to extract the angular frequency information  $\omega^+t$  of the connected distribution system through the phase locked loop (PLL).

$i_a, i_b$ , and  $i_c$  are the three-phase instantaneous current measurements. The sequence current vectors  $i_{abc}^+, i_{abc}^-$ , and  $i_{abc}^0$  can be obtained in a similar way as sequence voltages. Spatial rotations of  $2\pi/3$  and  $4\pi/3$  with respect to phase  $a$  are applied to phases  $b$  and  $c$  of the zero sequence components [15]. A new zero sequence current vector  $i_{abc}^h$  can be calculated as:

$$i_{abc}^h = \frac{1}{3} \begin{bmatrix} 1 & 1 & 1 \\ e^{j\frac{2\pi}{3}} & e^{j\frac{2\pi}{3}} & e^{j\frac{2\pi}{3}} \\ e^{j\frac{4\pi}{3}} & e^{j\frac{4\pi}{3}} & e^{j\frac{4\pi}{3}} \end{bmatrix} i_{abc}^0 \quad (1)$$

Therefore, the new zero sequence current vector  $i_{abc}^h$  has the same angular frequency and rotation frame as the positive sequence. Each current sequence vector ( $i_{abc}^+, i_{abc}^-$ , and  $i_{abc}^h$ ) can be transformed from  $abc$  coordinates into  $dq0$  coordinates by:

$$i_{dq0}^x = \frac{2}{3} \begin{bmatrix} \cos \theta_x & \cos\left(\theta_x - \frac{2\pi}{3}\right) & \cos\left(\theta_x + \frac{2\pi}{3}\right) \\ -\sin \theta_x & -\sin\left(\theta_x - \frac{2\pi}{3}\right) & -\sin\left(\theta_x + \frac{2\pi}{3}\right) \\ 0.5 & 0.5 & 0.5 \end{bmatrix} i_{abc}^x \quad (2)$$

where

$$\theta_x = \begin{cases} \omega^+t; & x = + \\ -\omega^+t; & x = - \\ \omega^+t; & x = h \end{cases} \quad (3)$$

and  $t$  is the time of system.

The pulse width modulation (PWM) signals can be obtained by applying proportional-integral (PI) control to each decoupled current component with the proper reference. The reference selection of each current component is discussed separately.

### A. Control System of Inverter

The objective of the inverter is to supply the loads with three-phase balanced voltage. Hence, the output voltages ( $v_{a,I}, v_{b,I}$ , and  $v_{c,I}$ ) of the inverter are measured to generate the references for each current component. The block diagram to generate current references for the inverter is shown in Fig. 3.  $v_{d,ref}^+$  is set based on the expected ac output voltage of the

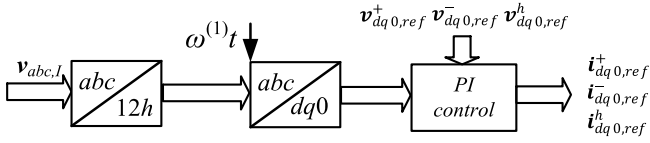


Fig. 3. Block diagram to obtain current references for an inverter.

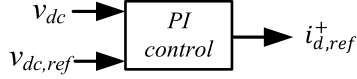


Fig. 4. Current reference generation block for the positive sequence of rectifier.

inverter. The other voltage references are set to zero to achieve a balanced output voltage with zero phase angle.

### B. Control System of Rectifier

There are two objectives for the rectifier in this paper. First is to transfer enough active power to the inverter. Second is to compensate negative and zero sequence currents at the substation transformer.

Positive sequence currents are responsible for the active power transfer from the substation to the inverter and maintain the dc voltage of the shunt capacitor at the dc bus. Hence, the references of the positive sequence currents are generated from the dc voltage feedback loop; see Fig. 4. The dc voltage and its reference are the inputs of the PI controller. The output of this PI controller is the reference of the  $d$ -axis current in the positive sequence  $i_{d,ref}^+$ . The references  $i_{q,ref}^+$  and  $i_{0,ref}^+$  are set to zero to achieve unity power factor of the positive sequence.

The purpose of demanding negative and zero sequence currents by the rectifier is to compensate the negative and zero sequence currents of the unbalanced load 1. The details of the compensation strategies (calculation of the references for the negative and zero sequence currents) depend on which measurements are available; see next section.

## IV. COMPENSATION OF NEGATIVE AND ZERO SEQUENCE CURRENTS

The simple system of Fig. 1 is chosen to illustrate the selection of references for the rectifier in the NSMG. By implementing the primary control policy described in Section III, the rectifier can be treated as an ideal linear element. Assume that the unbalanced load 1 is a constant current load with value  $I_1$  and all DG have merged into load 2 as an unbalanced P-Q load. In the following paragraphs, two secondary control methods are proposed to compensate the negative and zero sequence currents. The proposed secondary control policies can be seen as supplementary control strategies to the original secondary control system mentioned in [16]. From the point of view of compensation, the negative and zero sequence systems are similar. Thus, they are represented by a single superscript  $nz$ , such as  $I^{nz}$  for the negative or zero sequence current. The methods proposed below can be seen as a system reconfiguration performed by unbalancing the load.

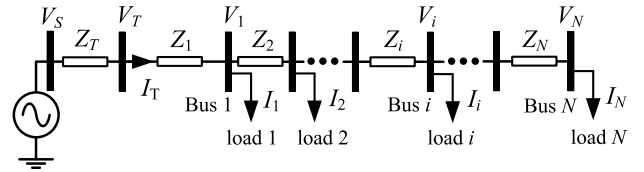


Fig. 5. Structure of a general radial system.

### A. Remote Current Compensation (RCC)

By applying Kirchhoff's Current Law (KCL) at bus 1 of the system in Fig. 1, we have:

$$\mathbf{I}_T = \mathbf{I}_1 + \mathbf{I}_R \quad (4)$$

where  $\mathbf{I}_T$  is the vector of three-phase complex currents flowing through the substation transformer. With remote communications, the measurement of  $\mathbf{I}_T$  is available at bus 2.  $\mathbf{I}_T$  can be decomposed into its sequence components by:

$$\begin{aligned} \begin{bmatrix} I_T^+ \\ I_T^- \\ I_T^0 \end{bmatrix} &= \frac{1}{3} \begin{bmatrix} 1 & e^{j\frac{2\pi}{3}} & e^{j\frac{4\pi}{3}} \\ 1 & e^{j\frac{4\pi}{3}} & e^{j\frac{2\pi}{3}} \\ 1 & 1 & 1 \end{bmatrix} \mathbf{I}_T \\ &= \frac{1}{3} \begin{bmatrix} 1 & e^{j\frac{2\pi}{3}} & e^{j\frac{4\pi}{3}} \\ 1 & e^{j\frac{4\pi}{3}} & e^{j\frac{2\pi}{3}} \\ 1 & 1 & 1 \end{bmatrix} \begin{bmatrix} I_{T,a} \\ I_{T,b} \\ I_{T,c} \end{bmatrix} \end{aligned} \quad (5)$$

where  $I_T^+$ ,  $I_T^-$ , and  $I_T^0$  are the complex sequence components of phase  $a$ . In a similar way each current vector can be decomposed into sequence components. Hence, (5) can be rewritten as:

$$\begin{bmatrix} I_T^+ \\ I_T^- \\ I_T^0 \end{bmatrix} = \begin{bmatrix} I_1^+ \\ I_1^- \\ I_1^0 \end{bmatrix} + \begin{bmatrix} I_R^+ \\ I_R^- \\ I_R^0 \end{bmatrix} \quad (6)$$

To balance the negative and zero sequence currents at the substation transformer, we set:

$$I_R^{nz} = -I_1^{nz} \quad (7)$$

where  $I_R^{nz}$  is the negative or zero sequence current of bus 2,  $I_1^{nz}$  is negative or zero sequence current of bus 1.

The rectifier references to eliminate the negative and zero sequence currents can be obtained from (6) and (7). For a general radial system where the NSMG is assumed to be installed at bus  $i$  (see Fig. 5), (7) is modified as:

$$I_i^{nz} = - \sum_{\substack{k=1 \\ k \neq i}}^N I_k^{nz} \quad (8)$$

In a real power system, all variables in (8) are correlated because the loads are mostly constant power. Therefore, the power flow changes as the input impedances of the NSMG change. At the same time, sudden changes of the NSMG impedances may cause transients in the entire distribution systems. Hence, instead of using (8) directly as the references for

negative and zero sequence currents, an iterative adjustment is proposed as follows (soft adjustment):

$$I_i^{nz}[j+1] = -K_p^{nz} I_T^{nz}[j] - K_i^{nz} \sum_{k=1}^{j-1} I_T^{nz}[k] \quad (9)$$

where  $I_i^{nz}[j]$  is the negative or zero sequence complex current of the NSMG at  $j^{\text{th}}$  iteration;  $I_T^{nz}[j]$  is the negative or zero sequence complex current of the substation transformer at the  $j^{\text{th}}$  iteration.  $K_p^{nz}$  and  $K_i^{nz}$  are constant control parameters. The adjustment action in each iteration step is done in steady state. The last term in (9) contains the past information of the transformer current. The iteration stops when the negative and zero sequence currents of the substation transformer are equal to zero or can no longer be reduced.

In a real application, (9) can be set as the current references of the NSMG. For time sequence power flow simulations without the dynamic model of the controlled converter, it is better to write (9) in its power form (following the principle of energy conservation) as:

$$S_i^{nz}[j+1] = 3V_i^{nz}[j]I_i^{nz}[j+1] \quad (10)$$

where  $S_i^{nz}[j]$  is the negative or zero sequence apparent power of the NSMG at the  $j^{\text{th}}$  iteration;  $V_i^{nz}[j]$  is the negative or zero sequence complex voltage of the NSMG at the  $j^{\text{th}}$  iteration.

To keep a constant active power transferred to the loads with no positive sequence reactive demand, we have:

$$S_i^+[j+1] = P_2 - \text{Re}[S_i^-[j+1]] - \text{Re}[S_i^0[j+1]] \quad (11)$$

where  $S_i^+[j]$ ,  $S_i^-[j]$ , and  $S_i^0[j]$  are the positive, negative, and zero sequence apparent powers of the NSMG at the  $j^{\text{th}}$  iteration, respectively;  $P_2$  is the active power demand of load 2 connected to the NSMG.

Neglecting the transient behavior of the NSMG in the time-sequence power-flow simulation, the converter in the NSMG can be treated as constant P-Q loads with the demands calculated from (10) and (11).

### B. Local Voltage Compensation (LVC)

Power engineers are always concerned with the cost of installing remote communication devices and their reliability. Hence, it is better to use local information to compensate the negative and zero sequence currents of the substation transformer when possible.

Applying Kirchhoff's Voltage Law (KVL) to the system of Fig. 1, we get:

$$\mathbf{V}_T = \mathbf{Z}_1(\mathbf{I}_1 + \mathbf{I}_R) + \mathbf{Z}_2\mathbf{I}_R + \mathbf{V}_R \quad (12)$$

where  $\mathbf{V}_T$  is the vector of three-phase complex voltages at the substation transformer,  $\mathbf{V}_R$  is the vector of three-phase complex voltages of bus 2.

Decomposing all parameters in (12) into sequence components, we have:

$$\begin{bmatrix} V_T^+ \\ V_T^- \\ V_T^0 \end{bmatrix} = \begin{bmatrix} Z_1^+(I_1^+ + I_R^+) \\ Z_1^-(I_1^- + I_R^-) \\ Z_1^0(I_1^0 + I_R^0) \end{bmatrix} + \begin{bmatrix} Z_2^+ I_R^+ \\ Z_2^- I_R^- \\ Z_2^0 I_R^0 \end{bmatrix} + \begin{bmatrix} V_R^+ \\ V_R^- \\ V_R^0 \end{bmatrix} \quad (13)$$

where  $V_T^+$ ,  $V_T^-$ , and  $V_T^0$  are the complex sequence components of unbalanced voltage  $\mathbf{V}_T$ ;  $V_R^+$ ,  $V_R^-$ , and  $V_R^0$  are the complex sequence components of unbalanced voltage  $\mathbf{V}_R$ ;  $Z_1^+$ ,  $Z_1^-$ , and  $Z_1^0$  are the complex sequence components of impedance  $\mathbf{Z}_1$ ;  $Z_2^+$ ,  $Z_2^-$ , and  $Z_2^0$  are the complex sequence components of impedance  $\mathbf{Z}_2$ .

To obtain the compensation references, we assume that the unbalanced load 1 has been balanced by  $I_R$ , hence the voltage at the substation transformer is balanced, expressed as:

$$V_T^{nz} = 0 \quad (14)$$

where  $V_T^{nz}$  is the complex negative or zero sequence voltage at substation transformer. Using (14) in (13) we can write:

$$I_1^{nz} = -\frac{Z_1^{nz} + Z_2^{nz}}{Z_1^{nz}} I_R^{nz} - \frac{1}{Z_1^{nz}} V_R^{nz} \quad (15)$$

To satisfy the assumption that  $I_T$  is balanced, we have:

$$I_T^{nz} = I_1^{nz} + I_R^{nz} = -\frac{Z_2^{nz}}{Z_1^{nz}} I_R^{nz} - \frac{1}{Z_1^{nz}} V_R^{nz} = 0 \quad (16)$$

yielding:

$$V_R^{nz} = -Z_2^{nz} I_R^{nz} = Z_2^{nz} I_1^{nz} \quad (17)$$

According to (16) and (17), the value of  $V_R^{nz}$  depends on the sequence impedance  $Z_2^{nz}$  when  $I_T$  is balanced. However, all the variables in (17) are unknown. When  $Z_2^{nz}$  is small,  $I_T$  can be nearly balanced by controlling  $V_R^{nz}$  to zero.

Without knowing the parameters of system,  $V_R^{nz}$  can be controlled to zero with an iterative process. The references of the negative sequence and zero sequence currents can be designed with the following iterative functions:

$$I_{R,ref}^{nz}[j+1] = -K_p^{nz} V_R^{nz}[j] - K_i^{nz} \sum_{k=1}^{j-1} V_R^{nz}[k] \quad (18)$$

where  $I_{R,ref}^{nz}[j]$  represents the negative or zero sequence current reference of the NSMG at the  $j^{\text{th}}$  iteration;  $V_R^{nz}[j]$  represents the negative or zero sequence voltage measurement of the NSMG at  $j^{\text{th}}$  the iteration. The last term in (18) contains the past information of the microgrid input voltage. The iteration stops when the negative and zero sequence voltages of the NSMG are equal to zero or cannot be reduced any further.

Suppose that  $V_R^{nz}[m]$  is zero after  $m$  iterations,  $I_T^{nz}[m]$  can be solved from (16). Therefore, we have:

$$I_T^{nz}[m] = -\frac{Z_2^{nz}}{Z_1^{nz}} I_R^{nz}[m] \quad (19)$$

Because  $I_1^{nz}$  can be solved from (16), the initial  $I_T^{nz}[0]$  can be calculated ( $I_R^{nz}[0]$  is zero):

$$I_T^{nz}[0] = I_1^{nz} = -\frac{Z_1^{nz} + Z_2^{nz}}{Z_1^{nz}} I_R^{nz}[m] \quad (20)$$

By comparing (19) and (20), the improvement after compensation can be obtained from:

$$\left| \frac{I_T^{nz}[0] - I_T^{nz}[m]}{I_T^{nz}[0]} \right| = \left| \frac{Z_1^{nz}}{Z_1^{nz} + Z_2^{nz}} \right| \quad (21)$$

According to (21), the improvement after compensation largely depends on the ratio between  $Z_1$  and  $Z_2$ . If the ratio is smaller than 1 ( $Z_1$  is smaller than  $Z_2$ ), the improvement is smaller than 50%.

For the radial system in Fig. 5, we have:

$$V_i = V_T - \sum_{k=1}^i \left( I_k \sum_{l=1}^k Z_l \right) - \sum_{k=i+1}^N I_k \cdot \sum_{k=1}^i Z_k \quad (22)$$

Compensating the negative and zero sequence voltages of the NSMG to zero at the  $m^{\text{th}}$  iteration, yields:

$$I_T^{nz}[m] = \sum_{k=1}^{i-1} I_k^{nz} - \frac{\sum_{k=1}^{i-1} \left( I_k^{nz} \sum_{l=1}^k Z_l^{nz} \right)}{\sum_{k=1}^i Z_k^{nz}} \quad (23)$$

From (23) one can conclude that: 1) the unbalanced currents at the substation transformer can be compensated using local voltage compensation at the NSMG; 2) the load currents downstream of NSMG ( $I_{i+1}$  to  $I_N$ ) can always be compensated by local voltage compensation. Note that (23) is presented to validate the improvements of the LVC method, but it is not used during the compensation process; therefore the estimation of the line impedances is not needed.

In a real system, the load may not behave as a constant current. As a result, the final sequence currents of substation transformer may not exactly follow (19) or (23), but compensation in steps is always effective.

According to the iteration equations (9) or (18), only the information at the substation or local bus is required. Hence, the proposed methods are independent from other phase balancing devices. If other load balancing devices exist, the proposed methods will share the compensation burden with those devices. Finding an optimal cooperation strategy is an interesting problem (design of a tertiary control policy), which is beyond the scope of a first paper on exploiting the balancing ability that microgrids offer.

## V. LIMITATION CONSIDERATIONS

Theoretically, the currents flowing through the transformer  $I_T$  can be balanced given enough information. The calculation time and the transient time for the converter to adjust are not a problem for balancing steady state currents. However, there are two major limitations that are discussed below.

### A. Limitation of the Measurements

The method proposed in Section IV needs to calculate the sequence components of voltages and currents. In distribution systems, power is transferred by the positive sequence components. Hence, the values of the negative and zero sequence components are much smaller than the positive sequence components in steady state operation.

When the negative and zero sequence components are larger than certain value  $\varepsilon$ , the measurement errors can be removed by taking multiple measurements and averaging. To reduce the impact caused by measurement errors and small oscillations when sequence voltage and current are small, a dead zone of unbalance compensation needs to be defined. If the negative

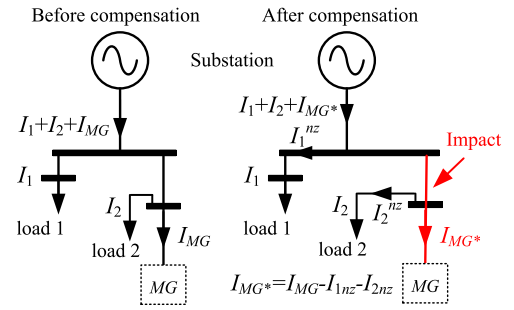


Fig. 6. The impact of distribution system by unbalance compensation.

and zero sequence components are smaller than  $\varepsilon$ , the NSMG stops adjusting its currents.

### B. Limitation of the Microgrid Capacities

The essence of current balancing is three-phase load balance. Under the control strategy proposed in Section IV, the NSMG balances the load of an entire system by adjusting its own three-phase power demands. To accomplish full compensation the capacity of the NSMG should be equal to the loads connected to microgrid plus the maximum unbalance downstream of the substation. However, the capacities of the NSMGs are normally limited by the size of the feeders supplying power or the power electronics elements in the converter.

Consider the system shown in Fig. 6, loads 1 and 2 are unbalanced constant current loads. Before compensation, the current at the substation is equal to  $I_1 + I_2 + I_{MG}$  which is unbalanced. After compensation, currents  $I_1$  and  $I_2$  do not change. Hence, loads 1 and 2 do not see any impact from the compensation process. However, the negative and zero sequence currents still exist in loads 1 and 2 which are now supplied by the microgrid (and not by the source). Thus the current of the microgrid becomes unbalanced. The feeder connecting the microgrid is the only one that is impacted by the compensating actions of the NSMG (which could be positive or negative).

Hence, there is an upper boundary in the capacity to regulate power demand of NSMGs which depends on the power handling capabilities of the devices involved. As a result, the currents at the substation transformers may not be perfectly balanced by a single NSMG when the system is highly unbalanced. The larger the rating of the dc capacitor and the power electronics elements, the better compensation can be achieved.

## VI. EXAMPLES

Two examples are presented in this section. The first example is the transient simulation based on Matlab to validate the ability of non-synchronous microgrids to function as a compensator and supplier.

The second example is the steady state time-sequence simulation based on OpenDSS [17]. Two compensation methods and two limitations are considered in this example.

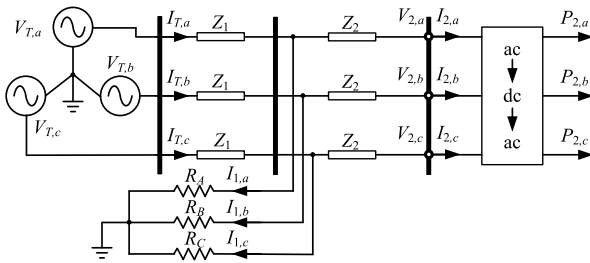


Fig. 7. Structure of the simplified system used for transient analysis.

TABLE I  
CONTROL PARAMETERS OF RECTIFIER

|     | Positive Sequence |      | Negative Sequence |      | Zero Sequence |      |
|-----|-------------------|------|-------------------|------|---------------|------|
|     | $d$               | $q$  | $d$               | $q$  | $d$           | $q$  |
| $P$ | 0.02              | 0.05 | 0.02              | 0.02 | 0.02          | 0.06 |
| $I$ | 0.1               | 0.1  | 0.1               | 0.1  | 0.2           | 0.8  |

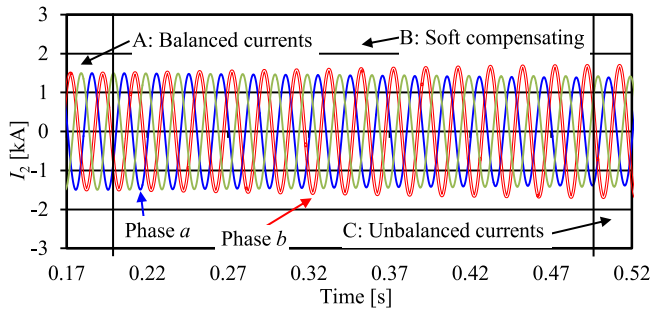


Fig. 8. Instantaneous current waveform of the NSMG.

### A. Transient Study for a Simplified System

Let us consider the system shown in Fig. 7, which runs at 50 Hz with  $Z_1 = Z_2 = 2 + j 5 \text{ m}\Omega$ .  $V_T$  is the three-phase balanced voltage source of 2.4 kV and zero phase angle. The unbalanced load 1 is modeled with different resistors per phase,  $R_A = 5 \Omega$  (2.3 MW),  $R_B = 10 \Omega$  (1.2 MW), and  $R_C = 5 \Omega$  (2.3 MW). The voltage at the dc bus is 4 kV and the three-phase load of the converter is 7.63 MW. The dc capacitor is 1.5 F. The control parameters of rectifier are given in Table I.

To show the normal operation conditions the average model of the converter is built in Matlab Simulink [18]. The control system of the rectifier is implemented according to Section IV. The function of unbalanced current compensation is accomplished with remote communications. Therefore, the converter of the NSMG at bus 2 can control its negative and zero sequence currents based on the information sent from bus 1.

There are three working stages of the NSMG for this transient study.

1) From  $t = 0$  to  $t = 0.2 \text{ s}$ , the NSMG operates in normal mode (not compensating). Thus, only positive sequence currents are demanded by the converter; see Fig. 8, region A. The instantaneous three-phase currents of the substation transformer are shown in region A of Fig. 9. In

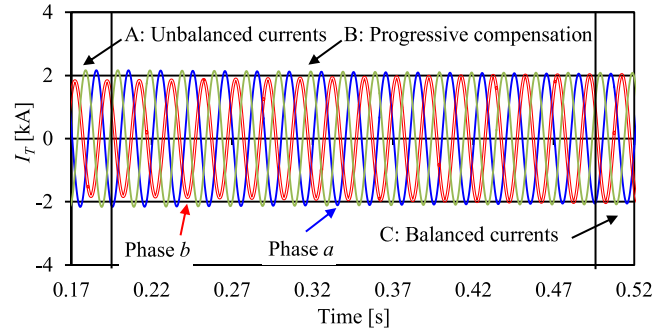


Fig. 9. Instantaneous current waveform at the substation transformer.

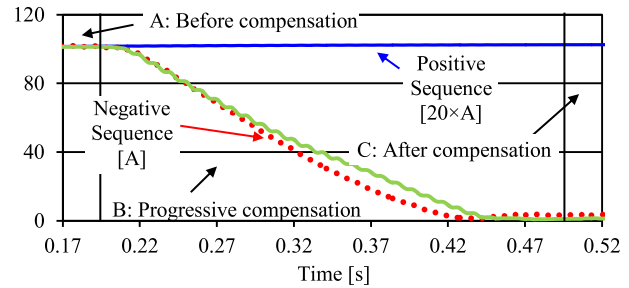


Fig. 10. Sequence current at the substation transformer.

this region, the three-phase currents of the transformer are unbalanced.

2) From  $t = 0.2 \text{ s}$  to  $t = 0.5 \text{ s}$ , the NSMG starts to compensate according to the information sent from bus 1 at  $t = 0.2 \text{ s}$ . To reduce the transient impact to the power system, the references of negative and zero sequence currents of the NSMG are gradually increased (similar to soft-start). According to region B in Fig. 8, the current amplitude of phase  $b$  increases and the current amplitudes of phases  $a$  and  $c$  reduce (at a slower pace). In contrast, Fig. 9 shows that the currents of the NSMG are becoming unbalanced as the currents at the transformer are compensated.

3) From  $t = 0.5 \text{ s}$  to  $t = 0.7 \text{ s}$ , the NSMG reaches a new steady state and keeps compensating the unbalanced currents of bus 1 until the next instructions are received; see region C in Fig. 8. Phase  $b$  of the rectifier consumes more power than phases  $a$  and  $c$ . This is to compensate the fact that phase  $b$  in load 1 consumes less power than the other two phases. To balance load 1, the NSMG needs to behave as an unbalanced load whose phase  $b$  carries more power.

The substation transformer currents are shown in Fig. 9. One can see that the unbalanced currents drawn by the NSMG very well compensate the unbalanced demand seen by the system source. Using communications, the substation transformer currents can be balanced near perfectly in less than 1 s.

The sequence components of the transformer current are shown in Fig. 10. In region B, the negative and zero sequence currents gradually decrease. The positive sequence current increases slightly to carry the energy transferred by the negative and zero sequence currents before compensation.

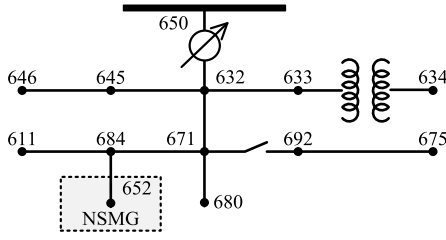


Fig. 11. IEEE 13-bus unbalanced system.

### B. Steady State Study of the IEEE 13-Bus System

A more complex system, the IEEE 13-bus system, is presented in this example. To implement the proposed control policy some modifications are needed:

1) To demonstrate the remote balancing ability of the NSMG, bus 652 (far from substation bus 650) is selected as the location of the NSMG.

2) To compensate the negative and zero sequence currents the lines connecting substation bus 650 downstream to bus 652 are modified to become three-phase.

3) Reactive power demand of bus 652 is assumed to be supplied by the NSMG [10]. Hence, only active power demand of bus 652 is considered. The three-phase active power demand of bus 652 is 128 kW.

The IEEE 13-bus system shown in Fig. 11 is unbalanced. The total demand of this modified system is  $S_{tot}$  is  $3662.6 + j1590.5$  kVA. The apparent power in phase  $a$  is  $1200.6 + j563.3$  kVA, the apparent power in phase  $b$  is  $1042.5 + j373.8$  kVA, and the apparent power in phase  $c$  is  $1420.1 + j653$  kVA.

Different from most methods described in the literature, which focus on compensation during a fault [14], the compensation proposed in this paper is applied in steady state. The NSMG located at bus 652 communicates with the substation bus 650 or measures the local information (voltages and currents) when the system is working in steady state. Based on the measurements or communication information from bus 650, the NSMG adjusts its currents demanded and waits for the system to stabilize. The time constant of a distribution system is much larger than the time constant of the NSMG (see example 1). Hence, the transient of the NSMG can be neglected.

The only constraint of the NSMG is the active power demand required by its load (when DG is not taken into account) which means:

$$P_{652}^+ + P_{652}^- + P_{652}^0 = P_{652} = 128 \text{ kW} \quad (24)$$

where  $P_{652}^+$ ,  $P_{652}^-$ , and  $P_{652}^0$  are the transferred active power by positive sequence, negative sequence, and zero sequence;  $P_{652}$  is the active power demand of the load supplied by the microgrid. According to the compensation methods proposed in Section IV, the results for each method are summarized in Table II. With communications and accurate measurements, the RCC method can balance the system perfectly. Based on only local information, the LVC method can reduce the current unbalance problem, but it is not eliminated.

TABLE II  
COMPENSATION RESULTS FOR RCC AND LVC METHODS

| Method        | Remote Information |       |          |       | Local Information |       |          |       |
|---------------|--------------------|-------|----------|-------|-------------------|-------|----------|-------|
|               | Zero               |       | Negative |       | Zero              |       | Negative |       |
| Sequence      | 0                  | 70    | 0        | 70    | 0                 | 110   | 0        | 180   |
| Iteration     | 0                  | 70    | 0        | 70    | 0                 | 110   | 0        | 180   |
| $I_{650}$ [A] | 43.0               | 0     | 58.5     | 0     | 43.0              | 3.7   | 58.5     | 40.5  |
| $I_{652}$ [A] | 0                  | 39.2  | 0        | 53.7  | 0                 | 36.1  | 0        | 64.6  |
| $V_{650}$ [V] | 0.01               | 0.001 | 0.07     | 0.003 | 0.01              | 0.002 | 0.07     | 0.048 |
| $V_{652}$ [V] | 57.9               | 4.8   | 39.2     | 23.8  | 57.9              | 0     | 39.2     | 0     |
| Control       | $K_p$              | $K_i$ | $K_p$    | $K_i$ | $K_p$             | $K_i$ | $K_p$    | $K_i$ |
| Parameter     | 0.04               | 0.1   | 0.03     | 0.08  | 0.07              | 0.08  | 0.1      | 0.1   |

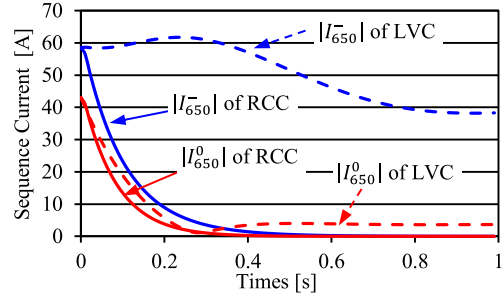


Fig. 12. rms value of negative and zero sequence currents under different compensation methods.

TABLE III  
INPUT POWER OF THE NSMG FOR RCC AND LVC METHODS

| Method                 | Remote Information |       |        | Local Information |       |        |
|------------------------|--------------------|-------|--------|-------------------|-------|--------|
|                        | $a$                | $b$   | $c$    | $a$               | $b$   | $c$    |
| Phase                  | $a$                | $b$   | $c$    | $a$               | $b$   | $c$    |
| $P$ [kW]               | 61.9               | 193.9 | -127.8 | -14.7             | 267.7 | -125.0 |
| $Q$ [kvar]             | -28.8              | 119.8 | -89.4  | -78.8             | 65.4  | 13.4   |
| $S$ [kVA]<br>(3-phase) | 128 + j1.6         |       |        | 128 - j0          |       |        |

The control parameters ( $K_p$  and  $K_i$ ) in Table II are selected to reduce the transient impacts on the distribution system. By applying the proposed control parameters into (9) and (18), the amplitude of current increments of each sequence are smaller than 5 A. Assume that the communication is continuous and the transient time constant of the NSMG adjusting its current is 10 ms. The compensating processes of the negative sequence and zero sequence currents are shown in Fig. 12. Without regulating the increment currents of the NSMG, the compensation process can be achieved within 100 ms.

The power demands of the NSMG before compensation and after compensation are shown in Table III. Both methods migrate active power from phase  $b$  to phase  $c$ , because the power demands in phase  $b$  of the entire system is below the average consumption and the power demands of phase  $c$  is above. The total active power consumptions of the NSMG in every adjustment is 128 kW which is satisfied with constraint (24).

As mentioned in Section V, the measurements may be imperfect in reality. To make the results more realistic, the limitations of measurement devices are considered. The accuracies of voltage and current measurements are considered as 0.2% [19]–[21]. Hence, the dead zones of voltage and current are defined as:

$$\varepsilon_V = V_{limits} = 2.4 \text{ kV} \times 0.2\% = 4.8 \text{ V} \quad (25)$$

TABLE IV  
COMPENSATION RESULTS FOR RCC AND LVC METHODS  
CONSIDERING THE LIMITATIONS ON MEASUREMENTS

| Method    | Remote Information |       |          |       | Local Information |       |          |      |
|-----------|--------------------|-------|----------|-------|-------------------|-------|----------|------|
|           | Zero               |       | Negative |       | Zero              |       | Negative |      |
| Sequence  | 0                  | 70    | 0        | 70    | 0                 | 60    | 0        | 60   |
| Iteration | 0                  | 70    | 0        | 70    | 0                 | 60    | 0        | 60   |
| $I_{650}$ | 43.0               | 0.5   | 58.5     | 0.95  | 43.0              | 0.54  | 58.5     | 45.7 |
| $I_{652}$ | 0                  | 38.8  | 0        | 52.8  | 0                 | 39.1  | 0        | 72.4 |
| $V_{650}$ | 0.01               | 0.001 | 0.07     | 0.004 | 0.01              | 0.001 | 0.07     | 0.05 |
| $V_{652}$ | 57.9               | 4.2   | 39.2     | 23.8  | 57.9              | 4.8   | 39.2     | 4.8  |

TABLE V  
INPUT POWER OF NSMG FOR RCC AND LVC METHODS  
CONSIDERING THE LIMITATIONS OF MEASUREMENTS

| Method                 | Remote Information |          |          | Local Information |          |          |
|------------------------|--------------------|----------|----------|-------------------|----------|----------|
|                        | <i>a</i>           | <i>b</i> | <i>c</i> | <i>a</i>          | <i>b</i> | <i>c</i> |
| $P$ [kW]               | 61.0               | 191.6    | -124.6   | -21.0             | 291.9    | -142.9   |
| $Q$ [kvar]             | -28.0              | 118.7    | -88.9    | -91.4             | 70.8     | 19.3     |
| $S$ [kVA]<br>(3-phase) | 127.9 + $j$ 1.8    |          |          | 128 - $j$ 2.4     |          |          |

TABLE VI  
COMPENSATION RESULTS FOR RCC AND LVC METHODS  
CONSIDERING THE LIMITATIONS OF CAPACITY

| Method    | Remote Information |       |          |      | Local Information |      |          |      |
|-----------|--------------------|-------|----------|------|-------------------|------|----------|------|
|           | Zero               |       | Negative |      | Zero              |      | Negative |      |
| Sequence  | 0                  | 10    | 0        | 10   | 0                 | 5    | 0        | 5    |
| Iteration | 0                  | 10    | 0        | 10   | 0                 | 5    | 0        | 5    |
| $I_{650}$ | 43.0               | 23.3  | 58.5     | 34.5 | 43.0              | 31.3 | 58.5     | 58.0 |
| $I_{652}$ | 0                  | 17.9  | 0        | 21.5 | 0                 | 15.8 | 0        | 14.9 |
| $V_{650}$ | 0.01               | 0.008 | 0.07     | 0.04 | 0.01              | 0.01 | 0.07     | 0.07 |
| $V_{652}$ | 57.9               | 29.2  | 39.2     | 29.7 | 57.9              | 40.9 | 39.2     | 34.1 |

$$\varepsilon_I = I_{limits} = \left| \frac{S_{tot}}{3V} \right| \times 0.2\% = 555 \times 0.2\% = 1.1 \text{ A} \quad (26)$$

Based on the same process, the compensation results are summarized in Table IV. The final power demands of the NSMG under the two different methods are shown in Table V. Comparing the results in Table IV with the results in Table II, the final zero sequence currents in the two methods are compensated below 2% of the original zero sequence currents with dead zone implementation. However, the negative sequence current compensation result in LVC method is slightly more sensitive to the dead zone.

Finally, the capacity constraint is considered as another limitation of the NSMG. The maximum amplitude of current in each phase is reduced to 50 A. The corresponding compensation results are shown in Tables VI and VII.

According to Table VI, the compensation ability of the NSMG is noticeable weakened by capacity limitation. Using NSMG with relatively small capacity for compensating an entire system is not economical. The losses of the system increase when migrating large amounts of current to one phase according to Table VII.

When the substation currents are highly unbalanced, full compensation from a single microgrid may negatively affect three phase customers. However, most of the customers in distribution systems in North America are single-phase and the capacity of a single microgrid is limited (full compensation from a single source cannot be achieved in practice). Therefore, negative impacts to other customers would be insignificant.

TABLE VII  
INPUT POWER OF NSMG FOR RCC AND LVC METHODS  
CONSIDERING THE LIMITATIONS OF CAPACITY

| Method                 | Remote Information |          |          | Local Information |          |          |
|------------------------|--------------------|----------|----------|-------------------|----------|----------|
|                        | <i>a</i>           | <i>b</i> | <i>c</i> | <i>a</i>          | <i>b</i> | <i>c</i> |
| $P$ [kW]               | 46.2               | 108.3    | -26.8    | 15.6              | 108.0    | 4.08     |
| $Q$ [kvar]             | -7.8               | 52.4     | -41.6    | 16.6              | -36.0    | 18.7     |
| $S$ [kVA]<br>(3-phase) | 127.7 + $j$ 3      |          |          | 127.7 - $j$ 0.7   |          |          |

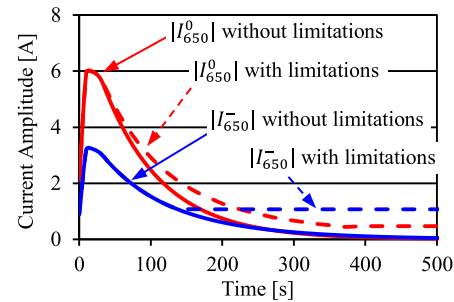


Fig. 13. Negative and zero sequence currents at substation transformer computed with time-sequence power-flow simulations.

Using a small NSMG unbalance compensation can be effectively applied in conjunction with static reconfiguration. Assume that the unbalanced IEEE 13-bus system has been balanced with the static reconfiguration method described in [7] and [8]. As the demand varies with time of day and season, the NSMG can provide dynamic compensation for these relatively smaller changes. Time-sequence power-flow simulations are performed to illustrate this. The active demand of phase *a* at bus 646 is assumed to increase 20% at  $t = 10$  ms. As a result, the system becomes unbalanced. It is not wise to re-configure the system using a static reconfiguration method for only for 20% of load increase at one bus. In this situation, the NSMG can provide the necessary compensation. Time-sequence power-flow simulations of the negative and zero sequence currents at the substation transformer are shown in Fig. 13.

According to Fig. 13, the system unbalance problem can be solved by the NSMG with the unbalanced compensation ability. At the same time, the total loss of system does not increase.

## VII. CONCLUSION

In this paper, a novel control strategy for phase balancing using non-synchronous microgrids is proposed. A control policy for converters working under normal and severe unbalanced condition has been investigated. Based on the typical control policy, two possible methods to implement the compensation function are presented: with and without remote communications.

With remote communication devices, the NSMG can compensate the current at the substation transformer perfectly. With only local information, the NSMG can still reduce effectively the unbalance problem at the substation transformer, but the unbalance is not completely eliminated.

Two numerical examples are provided to validate the control strategy with transient and steady state studies. By considering real-life limitations (measurement imprecisions and lack of communications), the balancing performance of the NSMG are established.

## REFERENCES

- [1] J. Zhu, M.-Y. Chow, and F. Zhang, "Phase balancing using mixed-integer programming," *IEEE Trans. Power Syst.*, vol. 13, no. 4, pp. 1487–1492, Nov. 1998.
- [2] P. S. Moses and M. A. S. Masoum, "Three-phase asymmetric transformer aging considering voltage-current harmonic interactions, unbalanced nonlinear loading, magnetic couplings, and hysteresis," *IEEE Trans. Energy Convers.*, vol. 27, no. 2, pp. 318–327, Jun. 2012.
- [3] J. Lu, F. Nejabatkhah, Y. Li, and B. Wu, "DG control strategies for grid voltage unbalance compensation," in *Proc. Energy Convers. Congr. Expo. (ECCE)*, Pittsburgh, PA, USA, 2014, pp. 2932–2939.
- [4] P.-T. Cheng, C.-A. Chen, T.-L. Lee, and S.-Y. Kuo, "A cooperative unbalance compensation method for distributed generation interface converters," in *Proc. Ind. Appl. Conf.*, New Orleans, LA, USA, 2007, pp. 1567–1573.
- [5] Y. Wang, L. Xu, and B. W. Williams, "Compensation of network voltage unbalance using doubly fed induction generator-based wind farms," *IET Renew. Power Gener.*, vol. 3, no. 1, pp. 12–22, Mar. 2009.
- [6] Y. Wang and L. Xu, "Coordinated control of DFIG and FSIG-based wind farms under unbalanced grid conditions," *IEEE Trans. Power Del.*, vol. 25, no. 1, pp. 367–377, Jan. 2010.
- [7] R. A. Hooshmand and S. Soltani, "Fuzzy optimal phase balancing of radial and meshed distribution networks using BF-PSO algorithm," *IEEE Trans. Power Syst.*, vol. 27, no. 1, pp. 47–57, Feb. 2012.
- [8] L. S. Czarnecki and P. M. Haley, "Unbalanced power in four-wire systems and its reactive compensation," *IEEE Trans. Power Del.*, vol. 30, no. 1, pp. 53–63, Feb. 2015.
- [9] Y. Xu, L. M. Tolbert, J. D. Kueck, and D. T. Rizy, "Voltage and current unbalance compensation using a static var compensator," *IET Power Electron.*, vol. 3, no. 6, pp. 977–988, Nov. 2010.
- [10] R. Saledo *et al.*, "Benefits of a non-synchronous microgrid on dense-load low-voltage secondary networks," *IEEE Trans. Power Del.*, to be published.
- [11] H. Kakigano, Y. Miura, and T. Ise, "Low-voltage bipolar-type dc microgrid for super high quality distribution," *IEEE Trans. Power Syst.*, vol. 25, no. 12, pp. 3066–3075, Dec. 2010.
- [12] T. Draglcevic, J. C. Vasquez, J. M. Guerrero, and D. Skrlec, "Advanced LVDC electrical power architectures and microgrids: A step toward a new generation of power distribution networks," *IEEE Elect. Mag.*, vol. 2, no. 1, pp. 54–65, Mar. 2014.
- [13] T. Hong and F. de León, "A reconfigurable auto-loop microgrid," *IEEE Trans. Power Del.*, vol. 30, no. 3, pp. 1644–1645, Jun. 2015.
- [14] Y. Suh and T. A. Lipo, "Control scheme in hybrid synchronous stationary frame for PWM AC/DC converter under generalized unbalanced operating conditions," *IEEE Trans. Ind. Appl.*, vol. 42, no. 3, pp. 825–835, May/Jun. 2006.
- [15] I. Vechiu, O. Curea, and H. Camblong, "Transient operation of a four-leg inverter for autonomous applications with unbalanced load," *IEEE Trans. Power Electron.*, vol. 25, no. 2, pp. 399–407, Feb. 2010.
- [16] IEEE Task Force on Microgrid Control, "Trends in microgrid control," *IEEE Trans. Smart Grid*, vol. 5, no. 4, pp. 1905–1919, Jul. 2014.
- [17] Simulation Tool—OpenDss. (2015). [Online]. Available: <http://smartgrid.epri.com/SimulationTool.aspx>.
- [18] J. Peralta, H. Saad, S. Denetiere, and J. Mahseredjian, "Dynamic performance of average-value models for multi-terminal VSC-HVDC systems," in *Proc. Power Energy Soc. Gen. Meeting*, San Diego, CA, USA, 2012, pp. 1–8.
- [19] Handbook of RITZ Instrument Transformers. (Feb. 2011). *Medium Voltage Instrument Transformers*. [Online]. Available: [http://www.ritz-international.com/fileadmin/pictures/download/RITZ-MediumVoltageInstrumentTransformers-Standard-Rev\\_Feb\\_2011.pdf](http://www.ritz-international.com/fileadmin/pictures/download/RITZ-MediumVoltageInstrumentTransformers-Standard-Rev_Feb_2011.pdf).
- [20] Handbook of Hioki Current Sensor. (Apr. 2014). *AC/DC Current Sensor CT6862, CT6863, 9709*. [Online]. Available: [https://www.hioki.com/products/recorder\\_logger\\_current/current\\_probes/1410](https://www.hioki.com/products/recorder_logger_current/current_probes/1410).
- [21] National Instruments Data Sheet. (Nov. 2014). *NI 9244 400 Vrms L-N, 800 Vrms L-L, Analog Input 3Ch Module*. [Online]. Available: <http://www.ni.com/datasheet/pdf/en/ds-527>.



**Tianqi Hong** (S'13) was born in Nanjing, China, in 1989. He received the B.Sc. degree in electrical engineering from Hohai University, China, in 2011, and the M.Sc. degree in electrical engineering from Southeast University, China, and the Engineering School, New York University (NYU), in 2013. He is currently pursuing the Ph.D. degree with the Engineering School, NYU.

His main interests are power system analysis, micro-grid, and electromagnetic design.



**Francisco de León** (S'86–M'92–SM'02–F'15) received the B.Sc. and M.Sc. (Hons.) degrees from National Polytechnic Institute, Mexico City, Mexico, in 1983 and 1986, respectively, and the Ph.D. degree from the University of Toronto, Toronto, ON, Canada, in 1992, all in electrical engineering.

He has held several academic positions in Mexico and has worked for the Canadian electric industry. He is currently an Associate Professor with the Department of Electrical and Computer Engineering, New York University. His research interests include

the analysis of power phenomena under non-sinusoidal conditions, the transient and steady-state analyses of power systems, the thermal rating of cables and transformers, and the calculation of electromagnetic fields applied to machine design and modeling.

Prof. de León is an Editor of the IEEE TRANSACTIONS ON POWER DELIVERY and IEEE POWER ENGINEERING LETTERS.